Electric Power Systems Research 228 (2024) 109981

Contents lists available at ScienceDirect

Electric Power Systems Research

journal homepage: www.elsevier.com/locate/epsr

Providing a combined solution to reduce very fast transient overvoltages in gas insulated substations

SeyyedAmirmohammad Mostafavi [a,*], SeyyedSajjad Mousavimajd [b]

[a] Department of Electrical Engineering, Arak University of Technology, Arak, Iran
[b] Department of Energy Engineering and Physics, Amirkabir University of Technology (Tehran Polytechnic), Iran

ARTICLE INFO

Keywords:
Very fast transient overvoltages
Gas high pressure substations
Nanocrystalline rings
XLPE cable
EMTP

ABSTRACT

The use of gas-insulated substations in high voltage levels of power systems is expanding due to its many advantages, such as the need for less space, resistance to environmental pollution, high reliability, and no need for continuous maintenance. One of the phenomena that threatens the insulation distances inside the closed enclosure in these substations is very fast transient voltages. These overvoltages are dangerous for the equipment inside the substation and connected to it as a result of the switching operation of gas-insulated substations, and if repeated, it can damage the internal insulation of the equipment. Also, these transient overvoltages in special cases such as extremely high voltages may cause serious damage to expensive substation equipment. Therefore, in this article, while examining the existing methods to limit very fast transient overvoltages in different and sensitive points of GIS substations, a new combined method based on the simultaneous use of nanocrystalline rings in the busbar and two XLPE cable paths, The direction of connecting the power transformer to the substation is provided. The results of the simulation on the 230 kV side of the GIS substation of Arak city show that the method proposed in this article has the lowest range of overvoltages compared to other methods. By using the proposed combined method, the range of very fast transient overvoltages in the power transformer terminal of the network under study is reduced by 60 % and this reduction can be seen in other points of the substation as well.

symbol	meaning of the symbol	unit
D_1	primary arc voltage range	Volt(V)
V_n	rated voltage of the power system	Volt(V)
D_2	voltage range in the last re-arc	Volt(V)
f	Frequency	Hertz (hZ)
τ'	Busbar delay time constant	-
R'	leakage resistance	Ohm(Ω)
C	Bus capacitor	Farad(f)
t_r	rise time of VFTO	Second (s)
k_t	constant of Toppler arc	-
$\left(\frac{E}{P}\right)_0$	The amplitude of the magnetic field intensity in the distance between the contacts	$\frac{860kV}{cm}$
h	of the field utilization factor	-
P	gas pressure	bar
L	Bus inductance	Henry (H)
Z	Bus wave impedance	Ohm(Ω)

(*continued on next column*)

(*continued*)

symbol	meaning of the symbol	unit
v	Traveling wave propagation speed in GIS	m/s
r	The outer radius of the conductor	cm
R	The inner radius of the GIS chamber	cm
r'	Fixed arc resistance	Ohm(Ω)
R_0	Resistance between contacts	Ohm(Ω)
τ	Delay time constant for gas insulation failure	-

1. Introduction

High pressure substations are essential facilities in power transmission networks. A common technology in the construction of substations is to use open space to install equipment and take advantage of the insulating properties of air. Providing land for the construction of a substation is very important from an economic point of view. In some cases, there is not enough land to build a substation in urban areas or in special conditions and places, or the price of land is very high; Therefore,

* Corresponding author.
E-mail addresses: a.mostafavi3024@arakut.ac.ir (S. Mostafavi), sajad.m@aut.ac.ir (S. Mousavimajd).

https://doi.org/10.1016/j.epsr.2023.109981
Received 10 August 2023; Received in revised form 5 October 2023; Accepted 1 November 2023
Available online 22 November 2023

saving in the use of land leads to a significant saving in the cost of implementing the project and makes it economical. One of the available options for reducing the size of substation is to create posts with gas insulation [1]. In these substations, unlike the substations with air insulation, sulfur hexafluoride gas has been used to create the required insulation distances between different phases and between the phase and the ground. SF6 gas is the only suitable insulator for use in GIS with high voltage level due to its excellent insulating properties and the electronegativity of its molecules [2]. In the last decade, the demand for installing GIS with high voltages in industrial areas has increased dramatically due to its advantages compared to AIS, including the need for less space, easy installation, employee safety, and less maintenance. Accordingly, according to the statistics of the Ministry of Energy of Iran, the trend of increasing the construction of GIS substations is growing, and according to the forecasts, the use of GIS substations in Iran can grow by 10 % between 2023 and 2035. But contrary to the advantages that GIS has over AIS, the emergence of very fast transient phenomena in GIS needs sufficient attention. Until the 1970s, all high-frequency transients of the power system were known as fast transients with a frequency range up to a few megahertz; But today, with the construction and use of GIS at very high and extremely high voltage levels, due to the new dimensions of these substations, transients with frequencies of several hundred megahertz have been reported in these substations [3, 4]. The main source of creating very fast transients in GIS is switching. Any insulation failure in the GIS leads to a very rapid increase in the voltage range in a very short period of time and propagates inside the GIS as traveling waves. Reflection of these traveling waves creates overvoltages with high amplitude. Insulation failure inside GIS due to sectioner operation or phase error with ground leads to very fast transient overvoltages [5]. There is no standard yet regarding VFTO amplitude and waveform; But according to the IEC60071-1 standard, these transients are in the highest frequency range (between 30 kHz and 100 MHz). These overvoltages lead to the destruction of the insulation of the equipment in GIS. Given that the dominant frequencies of VFTO are in the range of several MHz. have, it may match with the natural frequencies of the power transformer connected to GIS and as a result internal resonance occurs in the transformer [6]. So far, researchers have proposed different solutions, of course, few to reduce the mentioned overvoltages. For example, in Sree Chand et al. [7] it is proposed to use a parallel damping resistor in the VFTO damping direction switch. In Yiru et al. [8], by using the parallel resistance of the damper in the sectioner, the range of VFTO has been reduced. In Lijun et al. [9], ferrite rings have been tested in low voltage conditions and the results have been relatively good. However, their use in high voltage applications has led to complete saturation of these rings. By layering the ferrite rings, they can be prevented from being saturated at high voltages to a suitable extent. References [10–12] suggest the use of nanocrystalline rings to reduce VFTO. The alloy used to make nanocrystalline rings is based on iron with silicon and boron and other additives. Unlike ferrite rings, these materials are not saturated at high voltages. And they maintain their damping properties in very high voltages and very high field intensities. The nanocrystalline rings installed around the GIS conductors have further reduced the VFTO range. In the context of using nanocrystalline rings, reference [13] reports on a comprehensive study on a measurement method for the impedance characteristics in the frequency domain of magnetic rings as a function of DC-bias current up to saturation. The method and its key features are shown on an example of a nanocrystalline ring with large physical dimensions relevant for heavy power equipment. reference [14] presents a new model of a magnetic ring, employing full frequency-dependent characteristics of the ring's complex impedance, as well as the dedicated approach on modeling the saturation effect of the material magnetization characteristics. In reference [7], a high frequency electromagnetic amplifier is used to reduce the VFTO amplitude. High frequency amplifier design with low quality factor covers more frequency range. By adjusting the frequency range of the electromagnetic amplifier, the range of the VFTO has decreased with the dominant frequency of the VFTO. In Shah and Talati [15], the range of VFTO has been reduced by using combined L and T type RC filters. Also in Babaeilaktarashani [16], three RC filter structures with low impedance at high frequencies are introduced to reduce VFTO. In Abd-Allah et al. [17], the parallel capacitance at the terminal of the power transformer has been used to damp the VFTO in the substation design. The capacitor in arresters and capacitor voltage transformers or additional capacitors at the transformer terminal can be effective in reducing VFTO. In Abd-Allah et al. [17], 5 m of aerial cable are used at the terminal of the source side and 11 m of aerial cable are used at the terminal of the load side of GIS. The investigations carried out show the effect of the type of connector on the substation terminals. In Rao and Zameer [18] stated that the main part of VFTO damping occurred at the GIS terminal and in the OHTL overhead line connected between the GIS and the power transformer. Spreading VFTO on air-insulated lines and conductors reduces the VFTO peak time, and a longer air line between the GIS and the transformer further reduces VFTO in the power transformer. In reference Rao and Ramakrishna [19], the waveforms of VFTO at different speeds of the sectioner in 4 different modes have been investigated. The results have shown that the operation speed of the sectioner and the amount of stored load strongly affect the amplitude and rise time of the VFTO wave. In Babaeilaktarashani [16], by designing a suitable length for the bus ducts of the substation and choosing a suitable wave impedance for the GIS busbar, it has prevented the transmission of very fast transient overvoltages in a wide and high amplitude towards the power transformer. In Kuczek and Florkowski [20], connecting an XLPE cable to an overhead line has reduced the traveling waves caused by lightning strikes and switching. The results published in reference [21] show that the use of XLPE cable to connect the GIS to the power transformer has reduced the VFTO range at the power transformer terminal more compared to the overhead line and the gas line. Increasing the length of the cable further reduces the VFTO amplitude and transient damping occurs faster. In Han et al. [22], RC limiters have been used to protect power transformers against VFTO in parallel at the transformer terminal. Resistance absorbs VFTO energy and capacitor reduces VFTO frequencies. In Burow et al. [23], based on the simulation results, the use of LC low-pass filter at the pressure voltage level has been suggested as a new method to reduce VFTO. LC low-pass filter can be used to reduce overvoltages caused by lightning and switching in the network. In Liu et al. [24], the change in the voltage angle when the power switch is turned off has caused a change in the peak amplitude of overvoltage created in GIS; Therefore, switching off the switch at zero time or peak voltage can be very effective in the transient state created. It should also be mentioned that in GIS, a number of equipments are installed in the outer area of the substation. The use of protective wire to protect the equipment of the outer area against overvoltages caused by lightning striking the equipment or lines connected to the substation is a suitable method to prevent Creating a VFTO is in the substation.

However, research in this field is still ongoing. Therefore, in this article, a new combined method based on the simultaneous use of nanocrystalline rings in the busbar and XLPE cable at the end of the power transformer is proposed. The results of the simulation in the real 230 kV substation of Arak city have shown a greater reduction of this type of overvoltages using this method than other methods.

The organization of this article is as follows: in section (2) the types of transients in the power system have been examined. Section (3) has dealt with the modeling of the 230 kV substation in Arak city. In section (4) the proposed method is introduced and results The simulation of reducing the amplitude of very fast transient overvoltages will be shown in the study substation using EMTP-RV software. At the end, the conclusions and references are given in sections (5) and (6) respectively.

Table 1
Classes and shapes of overvoltages, Standard voltage shapes and Standard withstand voltage tests based on IEC60071-1 standard [24]

Class	Low frequency Continuous	Temporary	Slow front	Transient Fast-front	Very-fast-front
Voltage or overvoltage shapes	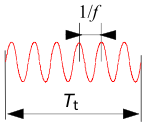	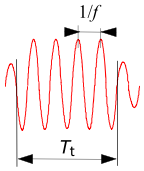	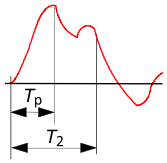	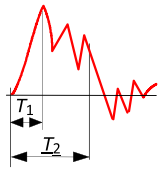	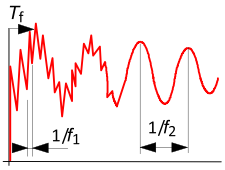
Range of voltage or overvoltage shapes	f = 50 Hz or 60 Hz Tt ≥ 3600 s	10 Hz < f < 500 Hz 0,02 s ≤ Tt ≤ 3600 s	20 μs < Tp ≤ 500 μs T2 ≤ 20 ms	0.1 μs < T1 ≤ 20 μs T2 ≤ 300 μs	Tt ≤ 100 ns 0.3 MHz < f1 < 100 MHz 30 kHz < f2 < 300 kHz
Standard voltage shapes	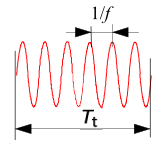 f = 50 Hz or 60 Hz Tt [a] f = 50 Hz or 60 Hz Tt [a]	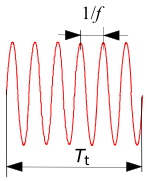 48 Hz ≤ f ≤ 62 Hz Tt = 60 s 48 Hz ≤ f ≤ 62 Hz Tt = 60 s	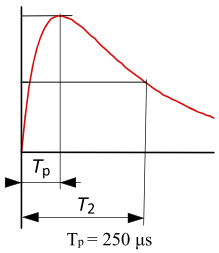 Tp = 250 μs T2 = 2500 μs Tp = 250 μs T2 = 2500 μs	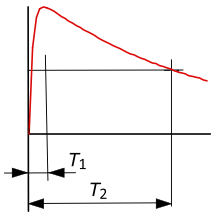 T1 = 1.2 μs T2 = 50 μs T1 = 1.2 μs T2 = 50 μs	a
Standard withstand voltage test	a	Short-duration power frequency test	Switching impulse test	Lightning impulse test	a

[a] To be specified by the relevant apparatus committees.

2. Transients in the power system

2.1. Classification of transients

Transients in the power system are divided into two categories, transients caused by lightning and transients caused by switching, in terms of their origin, and these transients are also defined in two standards, IEC60071-4 [25] and IEEE Std C37.122.1 [26] in terms of duration time and frequency range, have been expressed. According to the IEC60071-1 standard, transient overvoltages have a very short onset time of less than a few milliseconds and usually decay quickly. The types of overvoltages are classified according to this standard in Table 1 [24].

2.2. Very fast transient overvoltages in GIS

In GIS, the propagation of round-trip waves along the conductors is

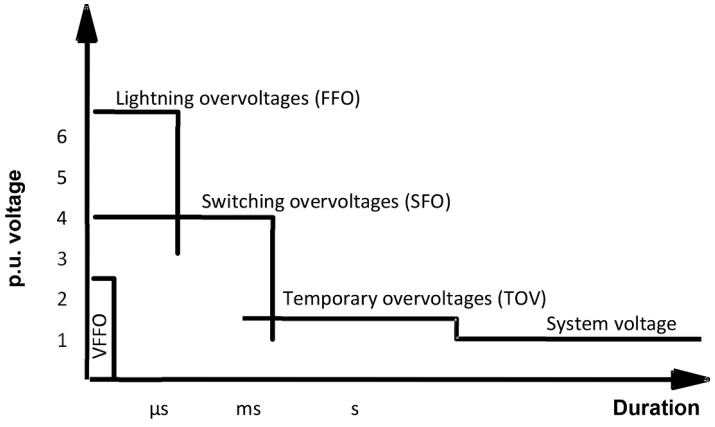

Fig. 1. Types of overvoltages and their types.

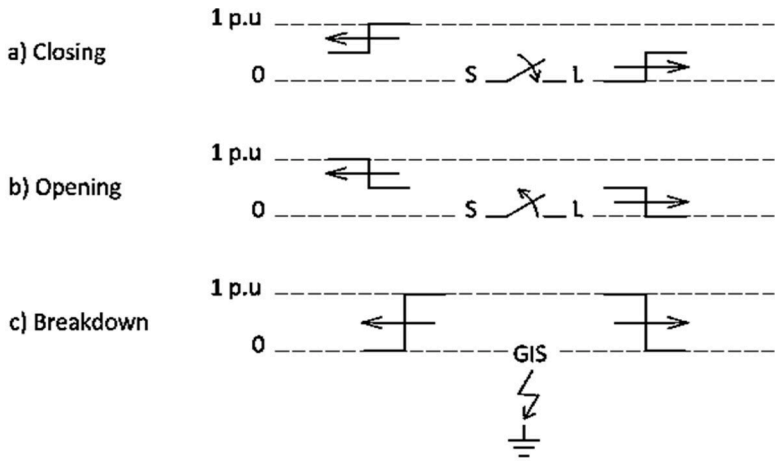

Fig. 2. Amplitude of traveling waves in the open and closed state of the switch and the phase error with the ground [16].

several times higher than in AIS. For this reason, switching transient overvoltages are more important in GIS than in AIS. The range of VFTO depends on the type of key and substation arrangement. Although the amplitude of the VFTO at ultra-high voltage levels is lower than the base dielectric level values; But the repetition of these overvoltages can significantly reduce the life of system insulators [25]. The range of transient overvoltages caused by switching is about 1.5 p.u to 2 p.u and may even reach up to 2.5 p.u During the operation of a normal sectioner, the worst case for creating a VFTO is when there is a voltage of 1 p.u on the source side and a voltage of –1 p.u on the load side of the sectioner. In these conditions, the maximum range of VFTO can reach 3 p.u The intensity of transient overvoltages in GIS increases with increasing voltage level and requires sufficient attention at voltage levels higher than 345 kV. Fig. 1 shows the diagram of overvoltage types and their range. According to Fig. 1, the amplitude of VFTO is less than 2.5 p.u The maximum range of VFTO for high voltage equipment in IEC and IEEE standards is lower than the basic insulation level [26].

The main reason for the formation of high-frequency VFTO in GIS is the switching function. The switching function includes opening and closing the power switch and sectioner. Due to the very slow operation speed of the sectioner contacts compared to the power switch, the primary arc occurs and new arcs are created. The generated traveling wave, based on the theory of traveling waves in transmission lines, propagates on both sides of the switch or the fault location [16]. According to Fig. 2, the operation of the sectioner in the contacts of its two sides has created a transient traveling wave with opposite polarity. The phase error with the ground causes the traveling wave to propagate with the same amplitude from the point of error generation on both sides of its generation location.

Traveling waves, based on the theory of traveling waves and with a speed close to the speed of light, are propagated along the GIS low conductors and due to reflections, a complex traveling wave is created. The complex traveling wave created creates larger overvoltages. After the operation of switching and creating traveling waves, these waves encounter discontinuities in their path and reach the points where the characteristic impedance of the path changes. At these points, the mobile waves are reflected and finally, by overlapping the reflected waves several times, the VFTO mobile waves are placed on the internal conductors of the GIS with great power [16]. Very fast transient overvoltages in GIS are divided into two categories: internal and external transients. Internal transients reduce the reliability of high pressure equipment such as transformers, insulators and protective equipment, external transients, by increasing the transient ground potential rise voltage or transient enclosure voltage, endanger the safety of substation workers. Traveling waves by creating very fast transient currents are the main source of creating electromagnetic fields in GIS and cause disturbances in the operation of control and protection equipment [16].

3. Modeling of 230/63 kV substation in Arak city

Due to the origin and mobile nature of the VFTO wave, GIS modeling should be done based on the compact equivalent circuit of elements or extensive line parameters. In general, elements with compact parameters are used in cases related to transients that propagate instantaneously at any point of the power system. In these cases, the behavior of the power system at the time of fault generation is described by ordinary differential equations. While in elements with extensive parameters, a time for the error wave should be considered. Therefore, the behavior of the system in this case is described by telegraph equations [16,25]. To model the internal effects of VFTO, only the internal mode between the main conductor and enclosure is considered and it is assumed that the metal enclosure is fully connected to the ground system. In the studies that intend to investigate the external effects of VFTO, a lossless transmission line model should be used to create the path of the grounded enclosure [27]. All the equipment in GIS is modeled based on the order of their placement in the single-line diagram of the substation, and the equipment inside the GIS hall is connected to other external equipment such as surge arresters, line traps, capacitor voltage transformers and transmission lines. Each section of GIS is modeled as a lossless transmission line with fixed parameters and with two important characteristics of wave impedance and wave travel time or wave propagation speed in EMTP software [28]. Due to the high frequency of VFTO, the capacitive capacity of equipment in GIS is more visible [29]. Since the three-phase system is symmetrical and each phase in this substation is located in a separate compartment, single-phase circuit has been used for GIS modeling. Each part of GIS can be modeled using physical length and propagation time or wave propagation speed in it and wave impedance [30]. According to the IEC62271-4 standard, the speed of wave propagation in GIS is about 0.95 to 0.96 of light propagation speed [31]. To model the equipment, three components of wave impedance, wave propagation speed and physical length of the equipment are considered. The VFTO wave propagation speed is equal to 285 m/μs [32]. If the equipment modeling accuracy is high; You can see more accurate values of the maximum VFTO range in different GIS points in the simulation.

Electric equivalent circuit includes compact and extended circuit elements. The substation conductors can be modeled by a piece of untransposed transmission line with extended parameters with wave impedance [33]. The wave impedance of GIS is between 60 and 75 ohms and less than the Airline transmission line with a wave impedance between 300 and 400 ohms. The wave impedance of XLPE cables is between 30 and 60 ohms and the speed of wave propagation in them is

Table 2
Modeling of gas substation equipment under study

Equipment	equivaleny circuit	Considerations
Bus Duct	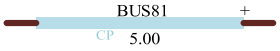	Lossless transmission line
Spacer		0.015 nF grounded capacitor
Surge arrester		Capacitor 0.2 nF
Line trap	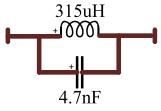	LC circuit (315 μH inductor and 4.7 nF capacitor)
Sectioner in general mode	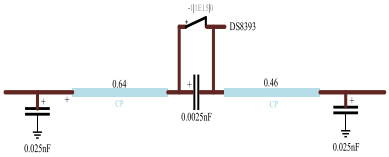	(lossless line 35 Ohms and 0.64 m on the source side), (lossless line 35 Ohms and 0.46 m on the load side), (0.0025 nF between contacts) and (0.025 nF with ground)
Circuit breaker in operation mode	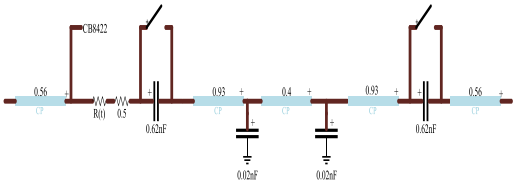	(lossless line 58 ohm and 0.56 m on the source side), (lossless line 58 ohm and 0.93 m on the load side), (lossless line 16 ohm and 0.4 m), (0.62 nF between contacts) and (0.02 nF with ground)
Arc model	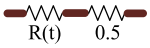	Fixed and variable resistance
Cable separator		Lossless line with 70 ohm impedance
Bushing (gas-air)	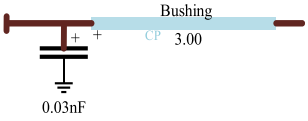	The wave impedance is 250 Ohms and the grounded capacitance is 0.03 nF on the air side
Power transformer	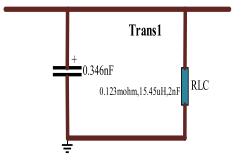	including grounded equivalent winding capacitor and bushing impedance
Current transformer	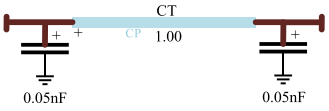	Equivalent circuit of π (70 ohm and 0.05 nF)
Capacitive voltage transformer	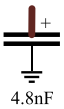	4.8 nF grounded capacitor

(*continued on next page*)

Table 2 (*continued*)

Equipment	equivaleny circuit	Considerations
Magnetic voltage transformer		0.1 nF grounded capacitor
Aerial cable	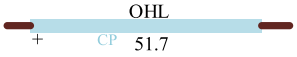	Lossless line with 350 Ohm impedance
XLPE cable	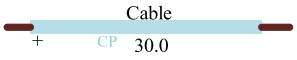	Lossless line with 30 Ohm impedance

between 0.33 and 0.6 of the speed of light. In this article, the study has been done only on very fast internal transients. To study a specific transient in the frequency range of 100 MHz, it is not necessary to model all components of the power system. For this reason, only the components that have a decisive influence in the transient high frequency range should be modeled [34]. VFTOs are generated in a GIS during disconnector or breaker switching operations, or by line-to-ground faults. In the switching operation in GIS, when the switch closes, the distance between two contacts reduces and the electric field between them will rise until sparking occurs. The first reignition of arc occurs when the voltage across contacts overreach the breakdown voltage of the gas insulation. The first strike occurs inescapably at the crest of the power frequency voltage, due to the slow operating speed. Thereafter, current flow through the spark and charge the capacitive load to the source voltage and the potential difference across the contacts falls and the spark will eventually quench. When switch closes, the highest amplitude of voltage oscillation happens at the first arc reignition [12]:

$$D_1 = \sqrt{\frac{2}{3}} V_n \tag{1}$$

where D_1 is the primary arc voltage range and Vn is the rated voltage of the power system. When switch opens, the behavior is a complete reversal of the closing operation. In this case, the highest amplitude of voltage oscillation appears at the last arc reignition [12]:

$$D_2 = \sqrt{\frac{2}{3}} V_n \left(1 + e^{\frac{-1}{\tau' f}}\right) \tag{2}$$

where D_2 is the voltage range in the last re-arc and f is the source frequency and τ' is the time constant of the busbar delay and according to the R' (leakage resistance) and C (capacitor) values of the substation busbar, it is obtained from Eq. (3) [35]:

$$\tau' = R' \cdot C \tag{3}$$

The rise time of VFTO depends on the intensity of the magnetic field in the distance between the contacts and the insulation breaking strength of SF6 gas and the coefficient h and is calculated from Eq. (4) [12]:

$$t_r = 13.3 \frac{k_t}{\left(\frac{E}{P}\right)_0 ph} \tag{4}$$

where $(\frac{E}{P})_0$ is equal to 860 $\frac{1kv}{cm}$. k_t constant of Toppler arc and SF6 gas pressure is higher than 5 bar. In spite of all furtherance in electrical measurement techniques and equipment, quantifying the VFTO at such high frequencies (a few MHz) is still challenging. The best way to measure the quantity of the VFTO is to investigate switching operation in GIS; however it can cause irreparable financial damages to the system. Thus, actual measurement in the GIS during operation is not feasible. Consequently, modeling techniques and appropriate assumptions can provide reasonable accurate predictions of the VFTO magnitudes and frequencies and their rate of rise [12].

Since VFTO contains substantially high frequency components ranging from hundreds of kHz to tens of MHz, most of the components have their capacitances dominating the other parameters [35]. Owing to VFTO's short time maintenance, when closing or opening disconnector switch or breaker in one phase, other phases cannot sense the transient wave. Thus, the three phases can be put into a single bus bar or separate bus bars.

Modeling of GIS is accomplished by utilizing electrical equivalent circuits put together by lumped elements and delineated by surge impedances and travelling times. The quality of simulation depends upon surge impedance and travelling times, and also on quality of the model of each separate GIS component.

The typical length of a GIS bus is much smaller than a conventional substation and since the VFTO is like a travelling wave of particular velocity with reflections and refractions, the bus bar can be represented by a constant parameter line with velocity v and surge impedance Z [36]. Relations (5) to (8) are also used to calculate the inductance, capacitance, wave impedance of GIS busbars and the propagation speed of traveling waves in GIS [12]:

$$L = \frac{\mu_0}{2\pi} \ln \frac{R}{r} \tag{5}$$

$$C = \frac{2\pi \varepsilon_r \varepsilon_0}{\ln \frac{R}{r}} \tag{6}$$

$$Z = \sqrt{\frac{L}{C}} = \sqrt{\frac{\mu_0 \ln^2\left(\frac{R}{r}\right)}{4\pi^2 \varepsilon_r \varepsilon_0}} = \sqrt{\frac{4\pi \times 10^{-7}}{4\pi^2 \times 1 \times 8.85 \times 10^{-12}}} \ln\left(\frac{R}{r}\right) \approx 60 \ln \frac{R}{r} \tag{7}$$

$$v = \frac{0.95}{\sqrt{L \cdot C}} \tag{8}$$

The values of L and C are the bus inductance and capacitance, respectively. r is the outer radius of the conductor, R is the inner radius of the GIS chamber, Z is the wave impedance of the bus, and v is the propagation speed of the traveling wave in the GIS.

When the key is closed in GIS, an electric arc occurs between the contacts. The mathematical relationship of variable arc resistance is in the form of relationship (9):

$$R(t) = r' + R_0 e^{\frac{-t}{\tau}} \tag{9}$$

where r' is the constant resistance of the arc and R_0 is the resistance between the contacts in the open state of the switch and τ is the delay time constant for the breakdown of the gas insulation. The resistance of the created arc decreases in a short time from a very high value of about 10^{12} ohms to a small value of about 0.5 ohms. In order to model the arc resistance, a fixed resistance equal to 0.5 Ohm has been used in series with a variable resistance that decreases exponentially [30].

According to the specifications of the equipment and maps related to the substation, the modeling of the equipment and finally GIS has been

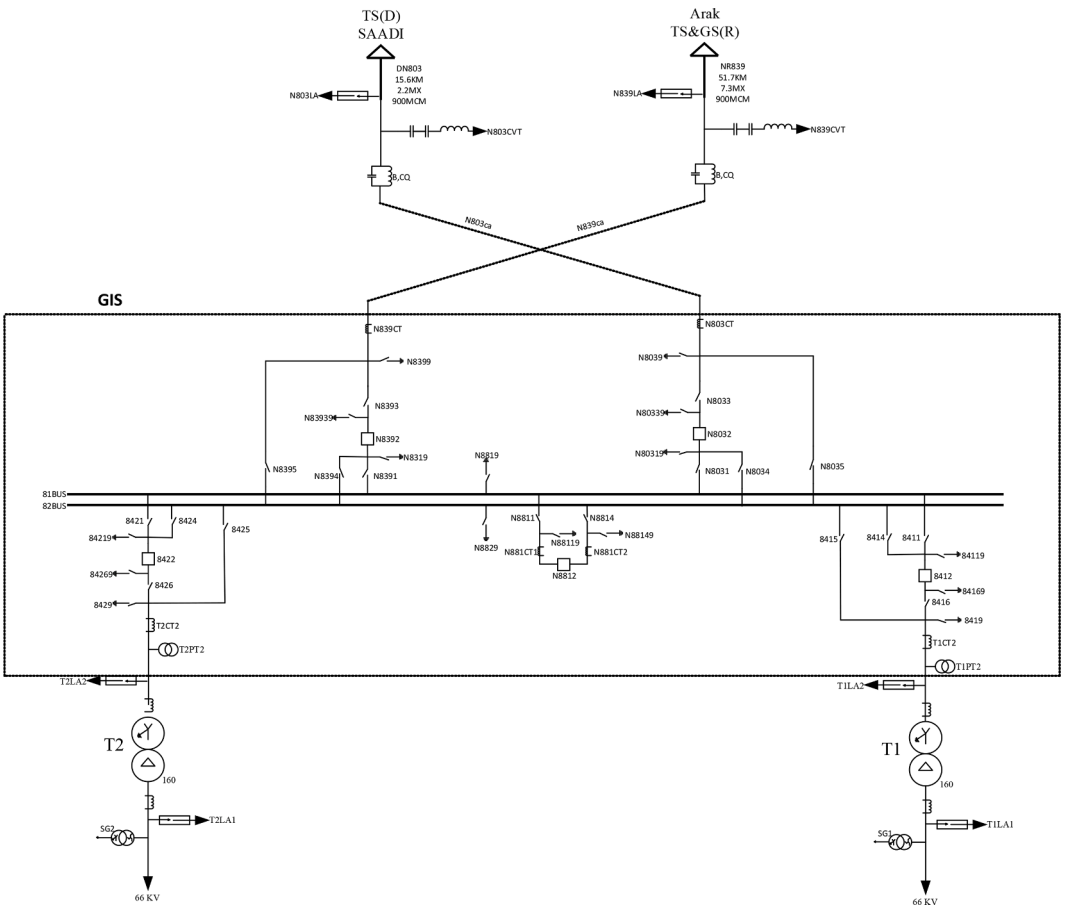

Fig. 3. Single line diagram of 230 kV substation in Arak city.

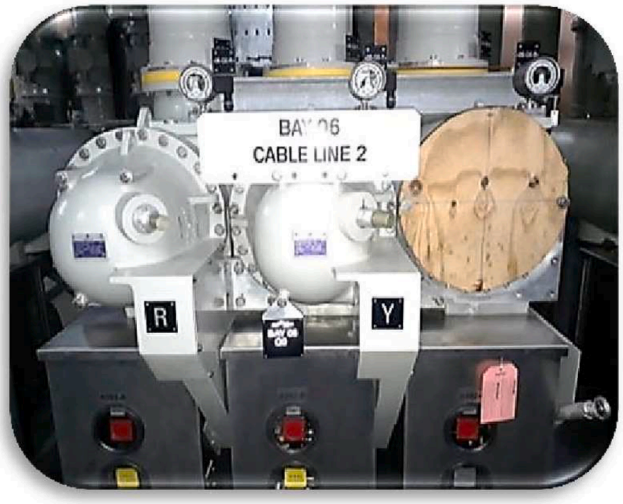

Fig. 4. Damaged switch in Arak gas substation.

done according to the models stated in Table 2.

4. Proposed method and simulation results

In this section, first, the 230/63 kV substation of Arak city, which is of GIS type with double busbar and is located in the north of Arak and near Arak University, is simulated. Two 230 kV lines from Arak combined cycle power plant and 230 kV Saadi substation are connected to this substation with two overhead transmission lines. The single-line diagram of 230 kV substation in Arak city is shown in Fig. 3. The equipment of this substation is placed one after the other like the substation with air insulation, and the power transformer is connected to the bus ducts of the substation with gas insulation by a 5 m long aerial cable path.

The equipment used in the 230/63 kV substation, on both the primary and secondary sides, are manufactured by AREVA. Two important factors of post arrangement and equipment and GIS modeling details affect the results of simulation and determination of VFTO range in GIS.

The line feeder associated with the combined cycle power plant and the transformer feeder are considered as the studied network; Because a real example of equipment destruction has been reported in this substation due to transient overvoltages caused by switching on the 8392 power switch. Fig. 4 shows a picture of the damaged switch due to the of switching in the gas substation of Arak city.

Fig. 5 shows the simulation of the studied part of the substation in the EMTP-RV software. The simulation for the operation of closing the line power switch (8392) in 1 μs and to be electrified busbar 81 and then closing the transformer power switch (8422) in 5 μs and to be electrified transformer number 2 has been done in EMTP-RV software. In this article, the waveforms related to the VFTO domain are examined in 4 important places, i.e. at the location of power switch 8392 (place1), busbar 81 (place 2), power switch 8422 (place3) and transformer number 2 (place4).

In order to achieve the best possible method and reduce the range of VFTO as much as possible, the methods that have caused the greatest reduction in previous studies are combined. The 9 combined methods reviewed in this article are as follows:

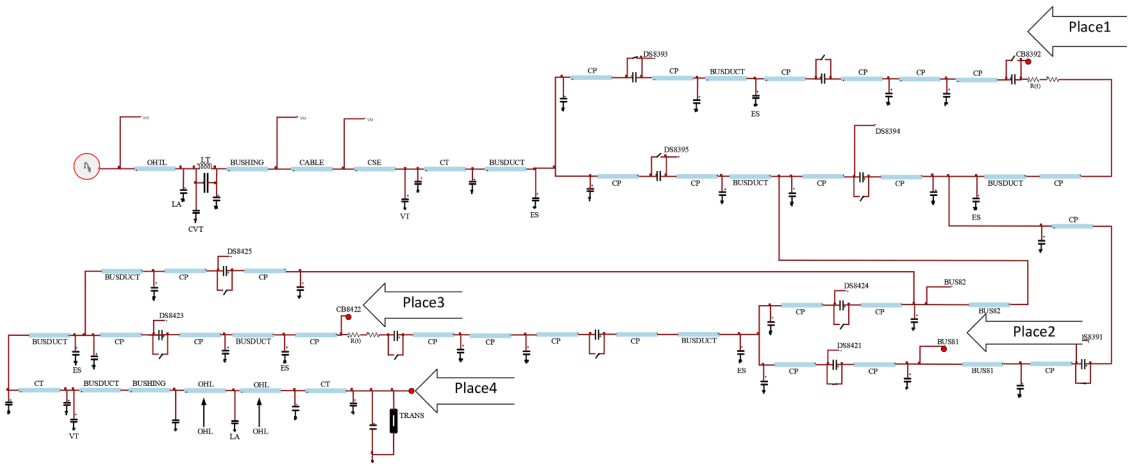

Fig. 5. The simulation circuit of the studied network in EMTP-RV software.

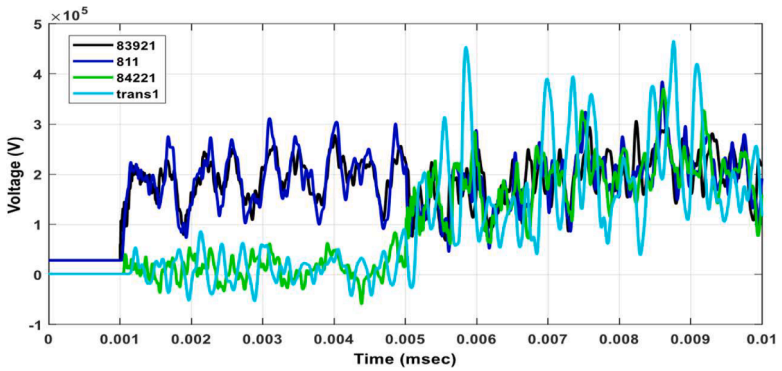

Fig. 6. The voltage waveform at different points of the substation of 230/63 kV in Arak city in the conditions without using limiting methods and without stored load.

1- The method of an XLPE cable route to connect the transformer to the substation [20].
2- The method of two rings of nanocrystals [10–12] - one path of the air line [16].
3- The method of two ferrite rings [9] - one overhead line path to connect the transformer [16].
4- The method of one ferrite ring [9] - one nanocrystalline ring [10–12] - one path XLPE cable [20].
5- The method of one ferrite ring [9] - one nanocrystalline ring [10–12] - two paths XLPE cable [20].
6- Method of two ferrite rings [9] - one path of XLPE cable [20].
7- The method of two nanocrystalline rings [10–12] - one route of XLPE cable [20].
8- Method of two ferrite rings [9] - two paths of XLPE cable [20].
9- Method of two nanocrystalline rings [10–12] - two paths of XLPE cable [20].

The simulation of each of the above methods has been done according to the arrangement of the equipment in Figs. 3 and 5 and using the modeling of Table 2 and with the help of EMTP-RV software. Thus, in the first method, only one XLPE cable route is used at the power transformer terminal instead of the aerial cable route. In the second method, two nanocrystalline rings and in the third method two ferrite rings are

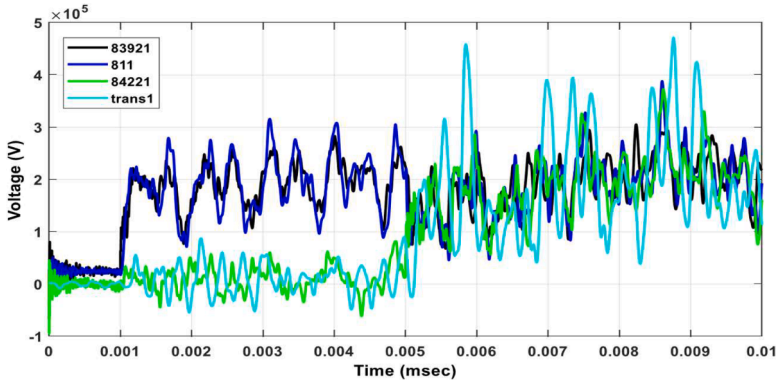

Fig. 7. Voltage waveform at different points of 230/63 kV substation in Arak city in the conditions without using limiting methods and with a stored load of 1 p.u.

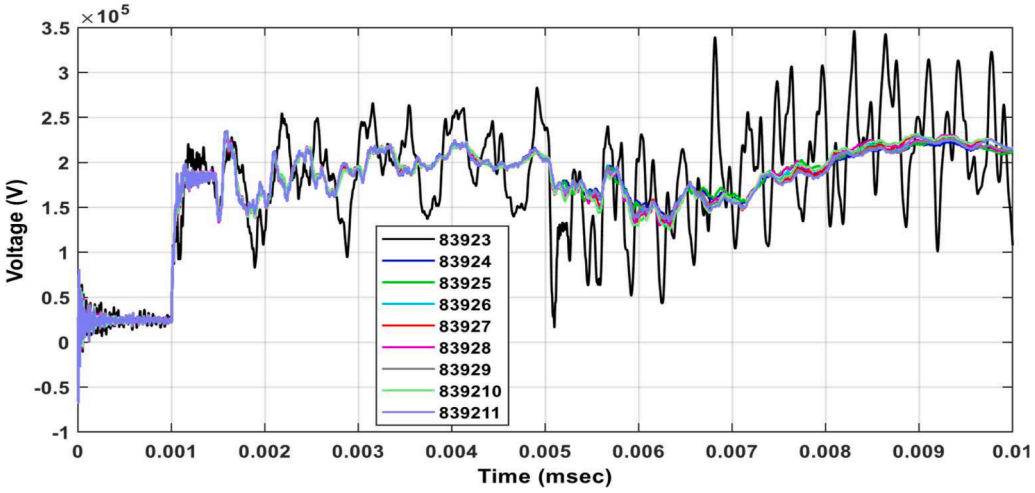

Fig. 8. VFTO range in place (1) for 9 combined methods in EMTP-RV software.

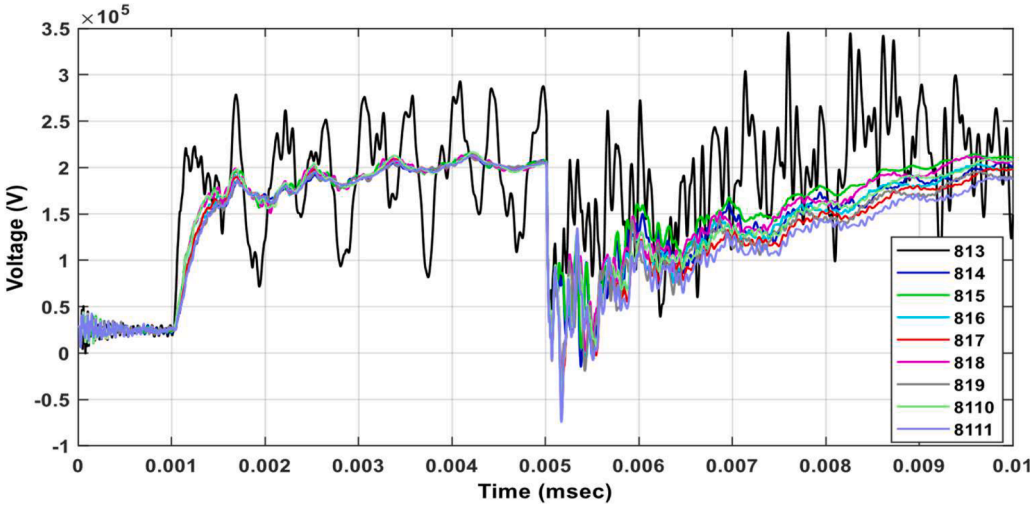

Fig. 9. VFTO range in place (2) for 9 combined methods in EMTP-RV software.

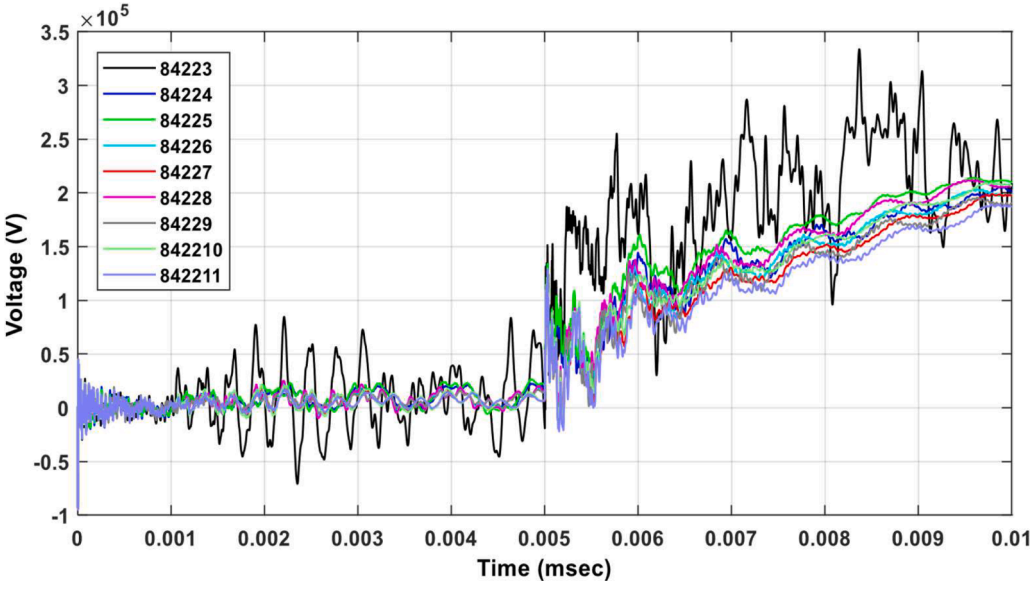

Fig. 10. VFTO range in place (3) for 9 combined methods in EMTP-RV software.

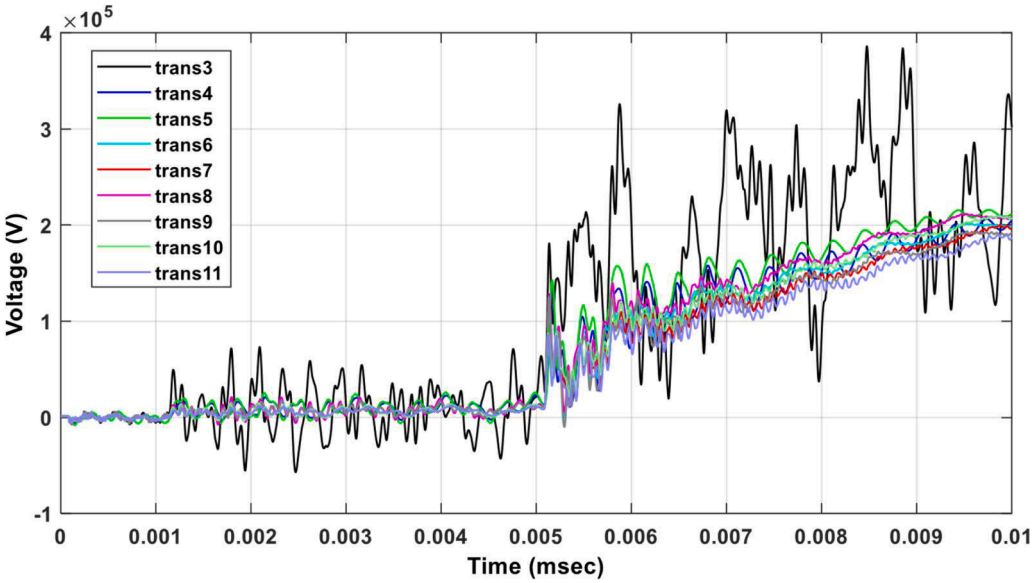

Fig. 11. VFTO range in place (4) for 9 combined methods in EMTP-RV software.

installed in each busbar. In the fourth method, a ferrite ring and a nanocrystal ring are simulated in each busbar and an XLPE cable path at the terminal of the power transformer. In the fifth method, a ferrite ring and a nanocrystal ring are installed in each busbar and two XLPE cable paths in the transformer terminal. In the sixth method, two ferrite rings are implemented in each busbar and an XLPE cable path is implemented at the transformer terminal. Also, in the seventh method, by installing two ferrite rings in each busbar, two XLPE cable paths are used at the transformer terminal. In the eighth method, two nanocrystal rings are installed in each busbar and an XLPE cable path is used at the transformer terminal. In the ninth method, in addition to installing two nanocrystal rings in each busbar, two XLPE cable paths are used at the power transformer terminal.

First, the studied network is simulated without using VFTO limiting methods and without residual load in EMTP-RV software, and the VFTO range obtained at 4 important points of the network is shown in Fig. 6.

Then the network is simulated without using the VFTO limiting methods and with a stored load of 1 pu on the load side of the 8392 and 8422 keys, and the range of VFTO obtained at the important points of the post is shown in Fig. 7.

In Fig. 6, in the case that no voltage limiting method is used (and without considering the remaining load), the voltage at place (1) is equal to 306.3 kV, at place (2) is equal to 384.7 kV, at place (3) is equal to 370.63 kV and in place (4) it is equal to 465 kV. In Fig. 7, considering the remaining load of 1 pu on the load side of the power switches and without applying limiting methods, the voltage in place (1) equals 305.3 kV, in place (2) equals 388.23 kV, in place (3) equals 372.9 kV and in place (4) it will be equal to 471.1 kV; Therefore, in the second case, due to the presence of the stored load, more overvoltage has been created in the studied network.

In order to reduce the range of these overvoltages in the substation, the use of the 9 combined methods mentioned in the studied network will be investigated, and the results of the simulation of all 9 methods will be analyzed in 4 important place.

Figs. 8–11 show the range of VFTO in places (1) to (4), respectively, for all 9 combined methods introduced in the EMTP-RV environment.

According to Fig. 8, the VFTO range at place (1) has been reduced from 305 kV to 234.5 kV using the combined method of two nanocrystal rings and two XLPE cable routes. According to Fig. 9, the VFTO range at place (2) has been reduced from 388 kV to 212 kV using the combined method of nanocrystalline double rings and two XLPE cable routes. The range of VFTO in place (3) by using the combined method of two

Table 3
Results of simulations performed using different methods

Combined methods to reduce VFTO	Place 1	Place 2	Place 3	Place 4
No limiting method and with 1 pu residual load	1.629	2	1.97	2.514
No limiting method	1.635	1.99	1.96	2.487
method one of XLPE cable to connect the transformer to the substation	1.815	1.856	1.76	2.075
Method of two nanocrystalline rings-one path of the air line	1.248	1.131	1.094	1.102
Method of two ferrite rings-one overhead line path for transformer connection	1.232	1.142	1.137	1.16
Method of ferrite ring-nanocrystalline ring-one path of XLPE cable	1.22	1.171	1.099	1.866
Method of ferrite ring-nanocrystalline ring-two paths of XLPE cable	1.218	1.158	1.066	1.065
Method of two ferrite rings - one path of XLPE cable	1.23	1.145	1.129	1.126
Method of two nanocrystalline ring - one path of XLPE cable	1.248	1.131	1.041	1.032
Method of two ferrite rings - two paths of XLPE cable	1.23	1.144	1.12	1.120
Method of two nanocrystalline rings - two paths of XLPE cable	1.248	1.128	1.005	1.013

nanocrystalline rings and two paths of XLPE cable, to connect the transformer to the substation, has the largest reduction, so that the range of VFTO has decreased from 372.9 kV to 189.03 kV This is clear in Fig. 10. Also according to Fig. 11, using the combined method of two nanocrystalline rings and two XLPE cable paths to connect the transformer to the substation, the range of VFTO decreased from 471 kV to 189.9 kV It was found that it has decreased by 60 % .

For a better review, the values of the VFTO range at different places of the substation, for all the methods reviewed in this article, according to per-unit , are given in Table 3. According to Table 3, it can be seen that the range of VFTO, in the case where two nanocrystal rings are used in each busbar, and two paths with two pieces of XLPE cable, to connect the transformer to the substation, has the highest voltage reduction compared to other methods We will have VFTO limiters. The block diagram comparing the simulation results of the combined methods of use is also given in Fig. 12, according to Fig. 12 it is clear that the combined method of simultaneous use of two nanocrystalline rings and two XLPE

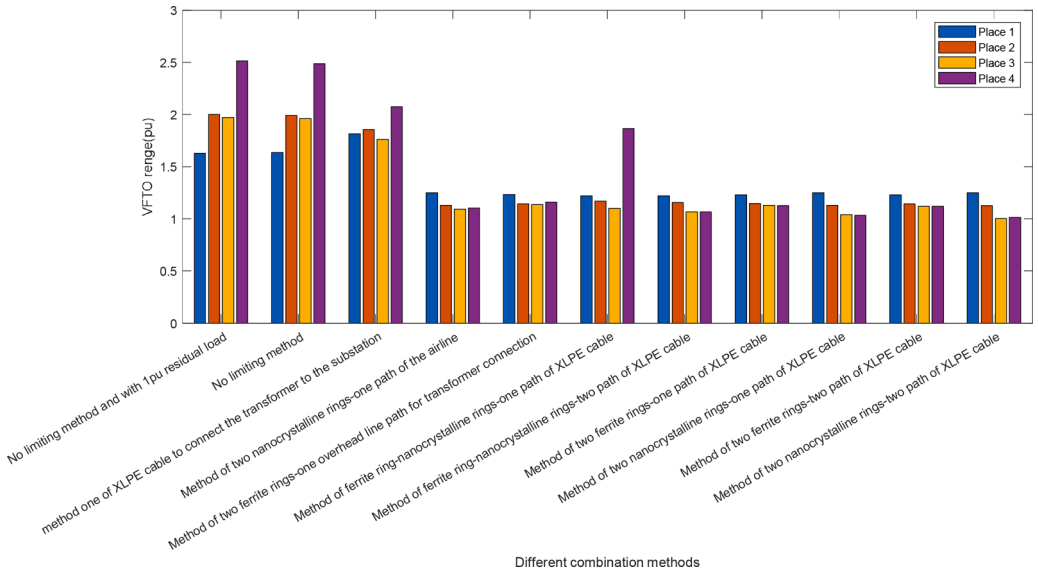

Fig. 12. Diagram comparing the results of simulations performed using different methods.

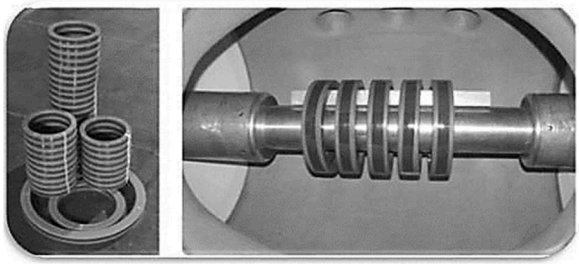

Fig. 13. Nanocrystalline rings and its application around the substation conductors.[29]

cable paths has the best result in reducing It is VFTO.

In the comparison analysis between the combined methods used to reduce the VFTO amplitude, the ferrite rings maintained their damping effect in the test conditions with low voltages; But at the level of high voltages, they may be completely saturated, and as a result, their damping properties are reduced to a marginal value. By layering the ferrite rings, they can also be used at high voltage levels; But layering of ferrite rings and adding epoxy resin material with low magnetic permeability between the layers reduces the effective magnetic permeability of the rings and as a result, the damping property of ferrite rings against VFTO is reduced [9]. The alloy used to make nanocrystalline rings is based on iron with silicon and boron and other additives. Using a technology of rapid solidification of molten materials, the liquid metal is turned into very thin strips with a thickness of about 200 μm, and the thin strip is twisted around the rings and subjected to a heat treatment with a temperature between 500 and 600 °C. It turns into the desired nanocrystalline state with very fine crystal grains. These materials have very special properties and have high magnetic permeability. The saturation flux density in these rings is very high. Unlike ferrite rings, these materials are not saturated at high voltages and retain their damping properties at very high voltages and field intensities [10–12]. According to Said et al. [21], which is a comparative analysis between aerial cables, XLPE cable and gas line to connect power transformer to GIS, in order to reduce VFTO. XLPE cable in the same length causes the greatest decrease in the range of VFTO, in the comparison between the gas line and the aerial cable, the gas cable reduces the range of VFTO more than the aerial cable.

In justifying the appropriateness of the proposed combined method, that is, the simultaneous use of two nanocrystalline rings and two XLPE cable paths, to connect the transformer to the substation, it can be concluded as follows: As mentioned in section (1), among the methods that are installed around the sub conductors, the greatest reduction in the VFTO range has been achieved by installing nanocrystalline rings in the busbar. These rings, like ferrite rings, are installed around the inner conductors of the GIS. The alloy used to make the rings is a nanocrystal based on iron with silicon and boron and other additives. These materials have very special properties and have high magnetic permeability. Also, the saturation flux density in these rings is very high. Unlike ferrite materials, these materials are not saturated at high voltages and they maintain their damping properties even in very high voltages and very high field intensity. Fig. 13 shows a picture of this type of rings around substation conductors.

According to the explanation of section (1), the more the number of nanocrystal rings installed around the sub conductors, the more the range of very fast transient overvoltages will decrease. But according to the references [34,17], the optimal number of nanocrystalline rings should be used around the substation conductors. According to numerous experiments with the number of nanocrystal rings of different types and types in the 230 kV substation of Arak city, the optimal number of nanocrystal rings for installation in each busbar has been obtained as 2, which reduces the range of very fast transient overvoltages With paying attention to the results stated in Table 3, it has reduced to a desirable level. Also, the use of XLPE cable to connect the power transformer to the substation, compared to the overhead cable and gas insulated line, has caused the greatest decrease in the VFTO range at the transformer terminal, and as the cable length increases, the VFTO peak values decrease. The reason for this is the XLPE cable's capacitance to ground, which effectively reduces the VFTO range. Therefore, by combining the two mentioned methods, i.e. by installing two nanocrystal rings in each busbar, and if two paths with two pieces of XLPE cable are used to connect the transformer to the GIS, the range of VFTO will be reduced the most at different points of the substation.

5. Conclusion

Due to the advancement of technology and the increasing use of GIS substations at the high voltage level, it is necessary to reduce transient overvoltages caused by switching in GIS substations. So far, various methods have been introduced to reduce very fast transient overvoltages. The methods used for busbar installation greatly reduce the

range of VFTO at different points of the substation. But the methods that are used in the transformer terminal reduce the VFTO amplitude more in the power transformer terminal and have less effect in reducing the VFTO amplitude in other parts of the substation. In this article, in order to obtain the method that has the greatest reduction in the amount of very fast transient overvoltages in all parts of a GIS substation, 9 different combined methods were proposed and reviewed. In order to check the effectiveness of each of these 9 methods, the real GIS substation of Arak city was implemented in the EMTP-RV software environment. 4 important places from this substation were selected to investigate the reduction of VFTO range. The simulation results of different combined methods, in this real substation, show that the simultaneous use of nanocrystalline rings in the busbar, and the parallel path of the XLPE cable in the terminal of the power transformer, in order to reduce the range of VFTO, in gas high pressure substations, can be the best and most effective method to reduce the range of VFTO as much as possible.

CRediT authorship contribution statement

SeyyedAmirmohammad Mostafavi: Conceptualization, Methodology, Software, Formal analysis, Data curation, Writing – original draft. **SeyyedSajjad Mousavimajd:** Validation, Investigation, Resources, Writing – review & editing, Visualization, Supervision.

Declaration of Competing Interest

The authors declare that they have no known competing financial interests or personal relationships that could have appeared to influence the work reported in this paper.

Data availability

The data that has been used is confidential.

References

[1] D. Moreira, M. Nunes, D. Moreira, D. Costa, Analysis of VFTO during the failure of a 550-kV gas-insulated substation, Electr. Power Syst. Res. 189 (2020), 106825.
[2] M. D'Souza, R.S. Dhara, R.C. Bouyer, Modularization of high voltage gas insulated substations, IEEE Trans. Ind. Appl. 56 (5) (2020) 4662–4669.
[3] I.A. Metwally, Technology progress in high-voltage gas-insulated substations, IEEE Potent. 29 (6) (2010) 25–32.
[4] P. Bolin, H. Koch, Introduction and applications of gas insulated substation (GIS), in: IEEE Power Engineering Society General Meeting, 2005, IEEE, 2005, pp. 920–926.
[5] T. Lei, H. Shen, W. Shi, P. Kang, Frequency analysis of measured transient voltage of neutral grounding reactor on UHV AC transmission line, in: 2020 IEEE International Conference on High Voltage Engineering and Application (ICHVE), IEEE, 2020, pp. 1–4.
[6] S.M. Al-Ameri, M.S. Kamarudin, M.F.M. Yousof, A.A. Salem, A.A. Siada, M. I. Mosaad, Interpretation of frequency response analysis for fault detection in power transformers, Appl. Sci. 11 (7) (2021) 2923.
[7] S.B. Sree Chand, T. Shanavas, N. Naufal, A review on transient analysis in Gas Insulated Substations, in: 2021 International Conference on Advances in Electrical, Computing, Communication and Sustainable Technologies (ICAECT), IEEE, 2021, pp. 1–5.
[8] W. Yiru, C. Guang, Z. Hao, Study on VFTO in UHV GIS substation, in: 2011 4th International Conference on Electric Utility Deregulation and Restructuring and Power Technologies (DRPT), IEEE, 2011, pp. 1756–1759.
[9] J. Lijun, Z. Yuanbing, P. Ge, Y. Zheng, Estimating the size of ferrite for suppressing VFTO in GIS, in: 2006 IEEE 8th International Conference on Properties & applications of Dielectric Materials, IEEE, 2006, pp. 388–391.
[10] N. Pathak, T. Bhatti, A. Verma, Mitigation/suppression techniques of very fast transient over voltages of a gas insulated substation, in: 2016 IEEE 1st International Conference on Power Electronics, Intelligent Control and Energy Systems (ICPEICES), IEEE, 2016, pp. 1–5.
[11] P.R. Reddy, J. Amarnath, Nanocrystalline To Suppress VFTO And VFTC For 245Kv Gas Insulated Substation, Int. J. Comput. Applic. 70 (13) (2013).
[12] S. Rahmani, A. Razi-Kazemi, Investigation of very fast transient over voltages in gas insulated substations, in: 2015 2nd International Conference on Knowledge-Based Engineering and Innovation (KBEI), IEEE, 2015, pp. 428–435.
[13] K. Kutorasiński, M. Szewczyk, M. Molas, J. Pawłowski, Measuring impedance frequency characteristics of magnetic rings with DC-bias current, ISA Trans. (2023).
[14] M. Szewczyk, J. Pawłowski, K. Kutorasiński, W. Piasecki, M. Florkowski, U. Straumann, High-frequency model of magnetic rings for simulation of VFTO damping in gas-insulated switchgear with full-scale validation, IEEE Trans. Power Deliv. 30 (5) (2015) 2331–2338.
[15] J.P. Shah, S. Talati, Modeling and analysis of very fast transient over-voltages in 400 kV GIS, in: 2019 8th International Conference on Power Systems (ICPS), IEEE, 2019, pp. 1–5.
[16] M. Babaeilaktarashani, A New Cost Effective Approach to Suppress Very Fast Transients on Power Transformers Connected to Gas Insulated Substations, Curtin University, 2016.
[17] M. Abd-Allah, A. Said, E.A. Badran, New techniques for VFT mitigation in GIS, J. Electr. Eng. (2014) 161–170.
[18] R.D. Rao and A. Zameer, "Estimation Of Vfto And Supression Methods In 420kv Gas Insulated Substation".
[19] J. Rao, A. Ramakrishna, Experimental study of effect of disconnector speed on very fast transient over voltages in a 420kV gas insulated substation, J. Electr. Syst. 16 (2) (2020).
[20] T. Kuczek, M. Florkowski, Modeling of Overvoltages in Gas Insulated Substations, ABB Corporate Research Center, Krakow, Poland, 2012.
[21] A. Said, E.A. Badran, M. Abd-Allah, Mitigation of very fast transient overvoltages at the more sensitive points in gas-insulated substation, Int. J. Electr. Eng. Inform. 4 (3) (2012) 414.
[22] B. Han, J. Lin, L. Ban, H. Wang, Z. Li, Z. Xiang, Simulation and test study on very fast transient overvoltage in 1000kV GIS substation, in: IOP Conference Series: Materials Science and Engineering 199, IOP Publishing, 2017, 012072.
[23] S. Burow, U. Straumann, W. Köhler, S. Tenbohlen, New methods of damping very fast transient overvoltages in gas-insulated switchgear, IEEE Trans. Power Delivery 29 (5) (2014) 2332–2339.
[24] S. Liu, Z. Xiong, H. Zhang, X. Li, J. Yang, Analysis of field circuit combination of GIS switching over-voltage, in: 2020 5th Asia Conference on Power and Electrical Engineering (ACPEE), IEEE, 2020, pp. 2204–2208.
[25] N.K. Challagondla, D. Thummapal, The study of very fast transient over voltages (VFTO) for the project of 400/220kV GIS substation with one and half circuit breaker configuration, in: 2016 IEEE International Conference on High Voltage Engineering and Application (ICHVE), IEEE, 2016, pp. 1–4.
[26] Y.S. Liew, Electrical Substation Design and Engineering, UTAR, 2019.
[27] J.D. Glover, M.S. Sarma, T. Overbye, Power System Analysis & Design, SI version, Cengage Learning, 2012.
[28] S. Burow, W. Köhler, S. Tenbohlen, U. Straumann, Damping of VFTO by RF resonator and nanocrystalline materials, in: 2013 IEEE Electrical Insulation Conference (EIC), IEEE, 2013, pp. 439–443.
[29] A.M. Dhaware, M. Potdar, Review on mitigation methods of very fast transient overvoltage in gas-insulated switchgear, Resincap Int. J. Sci. Eng 1 (2017) 20–25.
[30] R.D. Rao, Nanocrystalline based mitigation technique for very fast transient over voltages in gas insulated substations, Turk. J. Comput. Math. Educ. (TURCOMAT) 12 (2) (2021) 1025–1039.
[31] A.R. Ram, P. Swaraj, Suppression methods for very fast transient over-voltages on equipment of GIS, IJRET: Int. J. Res. Eng. Technol. ISSN (2012), 2319-1163.
[32] K. Prakasam, M. Surya Kalavathi, D. Prabhavathi, Mitigation and analysis of very fast transient over voltages (VFTOs) of transformer in 1000 KV Gas-Insulated Substation (GIS) using wavelet transform, in: Proceeding of International Conference on Intelligent Communication, Control and Devices: ICICCD 2016, Springer, 2017, pp. 69–88.
[33] R.D. Rao, M.S. Kalavathi, Suppression of very fast transient over voltages in gas insulated substations using RC filters, in: AIP Conference Proceedings 2519, AIP Publishing, 2022.
[34] N.N. Nam, A simple simulation model for Analyzing very fast transient over voltage in Gas Insulated switch gear, GMSARN Int. J. volume 12 (2018) 41–46.
[35] T. Lu, B. Zhang, Calculation of very fast transient overvoltages in GIS, in: 2005 IEEE/PES Transmission & Distribution Conference & Exposition: Asia and Pacific, IEEE, 2005, pp. 1–5.
[36] V.V. Kumar, J.M. Thomas, M. Naidu, Influence of switching conditions on the VFTO magnitudes in a GIS, IEEE Trans. Power Deliv. 16 (4) (2001) 539–544.